Diode-pumped multilayer Yb:YAG composite ceramic laser

To cite this article: F Tang *et al* 2012 *Laser Phys. Lett.* **9** 564

Abstract: All-ceramic multilayer composite ytterbium doped yttrium aluminum garnet (Yb:YAG) laser gain medium with doping concentration distribution of 0-5-10-15-20-15-10-5-0 at.% Yb ions was successfully fabrication by the technique of tape casting and simple vacuum sintering process. Full dense microstructure is achieved, and excellent optical properties are gained. The obtained result shows that the optical transmittance of >80% is reached when the wavelength is larger than 500 nm. The emission cross section is 4.03×10^{-20} cm^2 at the wavelength of 1030 nm. Continuous wave (CW) laser performance is further demonstrated when the sample is pumped by 940 nm fiber-coupler diode laser. The threshold absorbed pump power is 5.9 W, and the slope efficiency attains to 27% with transmission of output coupler of 6%.

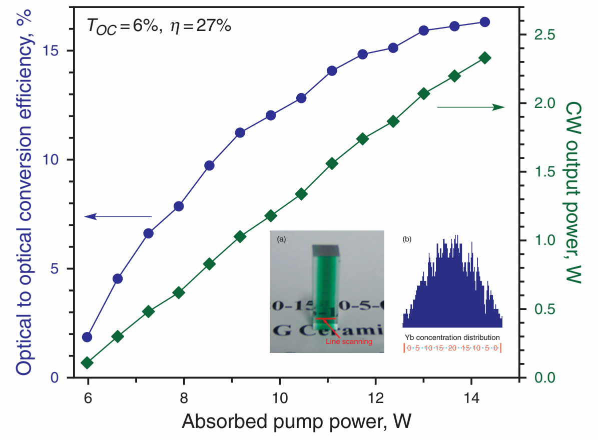

CW laser output power (solid rhombus) and optical efficiency (solid circle) of the Yb:YAG gradient composite ceramic sample as a function of absorbed pump power Inset figures are the photos of the unannealed ceramic (a) and Yb concentration distribution along thickness direction (b)

Diode-pumped multilayer Yb:YAG composite ceramic laser

F. Tang, [1,2] *Y.G. Cao,* [1,3,*] *J.Q. Huang,* [1] *W. Guo,* [1] *H.G. Liu,* [1] *W.C. Wang,* [3] *Q.F. Huang,* [1] *and J.T. Li* [1]

[1] Key Lab of Optoelectronic Materials Chemistry and Physics, Fujian Institute of Research on the Structure of Matter, Chinese Academy of Sciences, Fuzhou 350002, China
[2] Graduate School of the Chinese Academy of Sciences, Beijing 100039, China
[3] Department of Physics, Renmin University of China, Beijing 100872, China

Received: 2 April 2012, Revised: 18 April 2012, Accepted: 25 April 2012

Key words: Yb:YAG laser ceramic; all-ceramic composite; tape casting

1. Introduction

Ytterbium doped yttrium aluminum garnet (Yb:YAG) material has been well-known for its application of diode-pumped solid-state lasers due to its remarkable advantages, such as high quantum efficiency, absence of excited-state absorption, long fluorescence lifetime, and large emission bandwidth [1]. In the past decade, Yb:YAG ceramic laser has been successfully developed based on the advanced nanotechnology, as well as vacuum sintering technology [2–4]. It attracts more interest than single crystal counterpart because of low cost, high doping concentration, good mechanical properties, and easy fabrication of large-size/multilayer/multifunction specimen [5,6]. However, thermal effect is still problematic for efficient laser output. As we know, in monolithic laser materials with homogeneous dopant distribution, the exponential decay of the pumping intensity always causes tremendous longitudinal temperature gradients and thereby mechanical stress peaks during the laser operation process [7–9]. In order to solve this problem, the design of composite structure consisting of multi-layers with different doping level was proposed, and some investigations on this kind of composite

---

[*] Corresponding author: e-mail: caoyongge@fjirsm.ac.cn

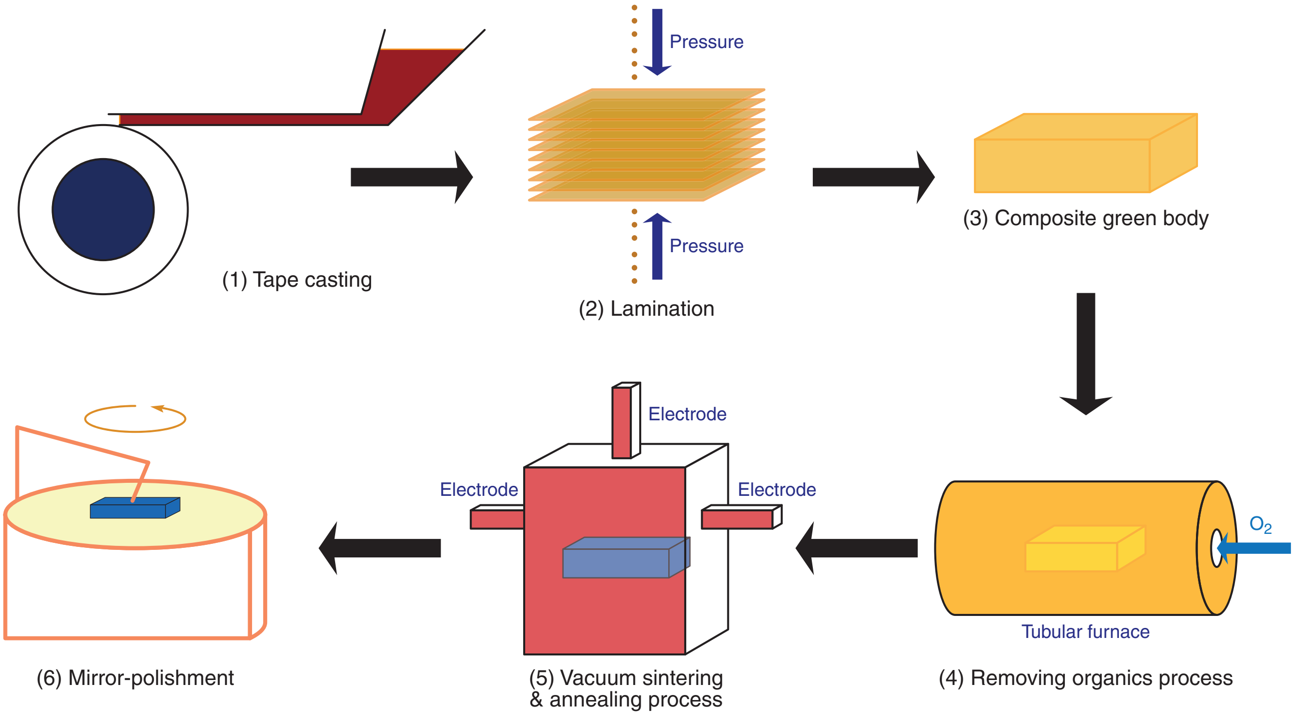

Figure 1 (online color at www.lasphys.com) Brief fabrication process of the Yb:YAG concentration gradient composite ceramic

laser ceramics have been carried out in recent years [10–14] Through these studies, it is found that the method of dry-pressing shows shortages in both the controlling of the thickness of single layer and the bonding between different layers and thereby inevitably influence the laser efficiency, while the combination of tape cast and hot-isostatic press (HIP) technology seems to be a new and efficient route for the exploration of composite laser materials. S.-H. Lee firstly reported Nd:YAG transparent ceramic fabricated by tape casting and HIP in 2009 [13], and N. Ter-Gabrielyan presented the first report on the successful fabrication of Er:YAG composite laser ceramic using the same method in 2010 [14] The biggest drawback of this method is the high fabrication cost originated from HIP process. Recently, we found that simple vacuum sintering technology can be used to replace HIP under the condition of the optimization of fabrication details [15], which can reduce the fabrication cost significantly.

In this letter, based on the technique of tape casting and simple vacuum sintering process, the successful fabrication of multilayer composite Yb:YAG laser ceramic with dopant concentration distribution of 0-5-10-15-20-15-10-5-0 at.% Yb along thickness direction was demonstrated, and the microstructure, spectroscopic characteristics and laser properties of this composite ceramic were studied too.

2. Experimental setup

The brief fabrication process, as shown in Fig. 1, is described as follows: high-purity powders of α-Al_2O_3, Y_2O_3, and Yb_2O_3 were weighted in accordance with the chemical composition of $(Yb_xY_{1-x})_3Al_5O_{12}$ ($x = 0, 5, 10,$ 15, and 20, respectively). Then, they were mixed in solvent with fish oil as dispersant. The used solvent was the mixture of ethanol and xylene. Followed by addition of plasticizers and binder, the slurries were second-milled. The obtained slurries were de-aired, and then cast to form thin tapes. These tapes were cut into pieces that were stacked and laminated into green parts. The organics in these parts were burned off in oxygen atmosphere prior to the following cold-isostatic press process. Sintering process was carried out at 1730°C for 20 h under vacuum condition of 10^{-7} Torr. The annealing treatment was carried out under oxygen atmosphere at 1450°C for 10 h. The annealed ceramic was then polished until the surface flatness achieved about $\lambda/10$ (λ is 632.8 nm). Finally, multilayer composite laser ceramic with the size of about $6\times5\times3.3$ mm^3 (the thickness of doping region was 2.2 mm) was obtained.

Optical transmittance was recorded by using UV/Vis/NIR spectrophotometers (PerkinElmer, Lamda 900) and the samples studied were detected ranging from 230 to 1100 nm. The fluorescence spectra and decay curves at 1030 nm were recorded using a spectrophotometer (Edinburgh, FLS920), when a microsecond flash lamp (Edinburgh, mF900) was used as the exciting source

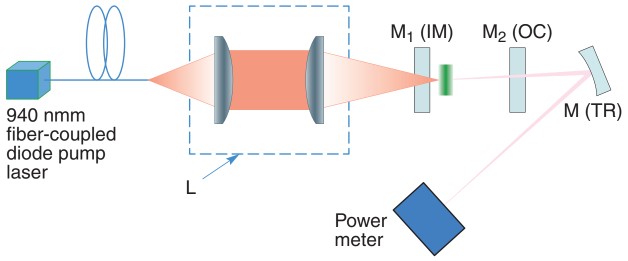

Figure 2 (online color at www.lasphys.com) Schematic diagram of experimental setup for laser-diode pumped Yb:YAG composite ceramic: L – coupling lens, M_1 – input mirror, M_2 – output coupler, and M – the total reflectivity at laser wavelength

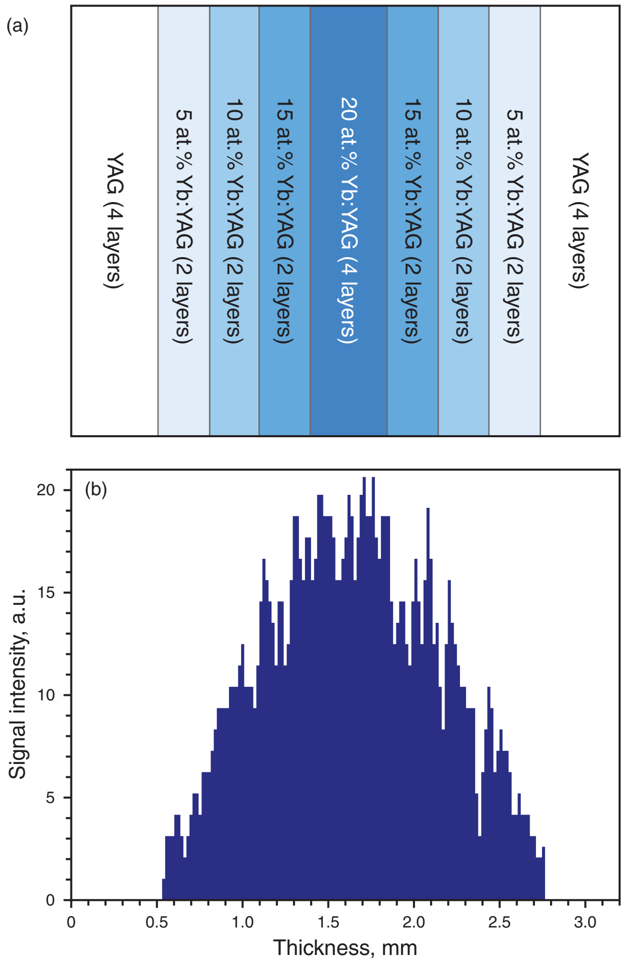

Figure 3 (online color at www.lasphys.com) (a) – design scheme and (b) – EDAX line scanning along doping thickness direction the concentration for the gradient Yb:YAG composite ceramic

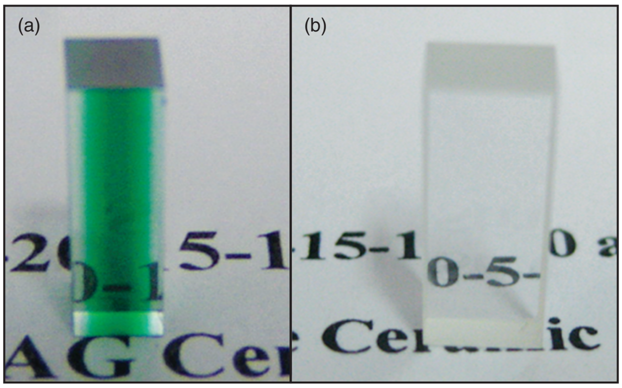

Figure 4 (online color at www.lasphys.com) Photos before (a) and after (b) annealing for the concentration gradient Yb:YAG composite ceramic

and the exciting wavelength was 940 nm. The signals were detected with a NIR PMT (Hamamatsu, R5509). The laser cavity of an end-pumped plano-plano resonator was used with total cavity length of about 35 mm, as shown in Fig. 2. Both surfaces of composite ceramic were AR-coated for pump and laser wavelength. Then, it was pumped by 940 nm fiber-couple diode laser, and the fiber core diameter was about 400 μm. Two convex lenses were used to focus the pump beam into the ceramic sample. The total cavity was mainly composed of two mirrors, the input mirror (IM) and output coupler (OC). The former has 95% transmission at 940 nm and 99.8% reflectivity at 1030 nm. Output coupler with transmission of 6% was used to measure laser performance. The composite ceramic was placed as close as possible to the input mirror and held on the brass mount. No special arrangement was taken to ensure good thermal contact or cooling of the composite.

3. Experimental results and discussion

The Design scheme of the sample (with concentration distribution of 0-5-10-15-20-15-10-5-0 at% Yb along thickness direction) is shown in Fig 3a The Yb doping level increases from laterals to the central region. As aforementioned, the design of such a composite structure is based on the consideration of effective thermal management during laser operation process. Fig. 3b gives experimental measurement of the distribution of Yb concentration along the cross-section by energy dispersive analysis of X-ray (EDAX) line scanning technology. It exhibits the increase of Yb concentration from laterals to the central region, which is consistent with the design scheme (Fig. 3a) Fig. 4a shows photos of the unannealed composite ceramic, and color variation can be clearly observed. Viewing from the cross-section, dark green is present at the central region (20 at% Yb:YAG), while the edges (pure YAG)

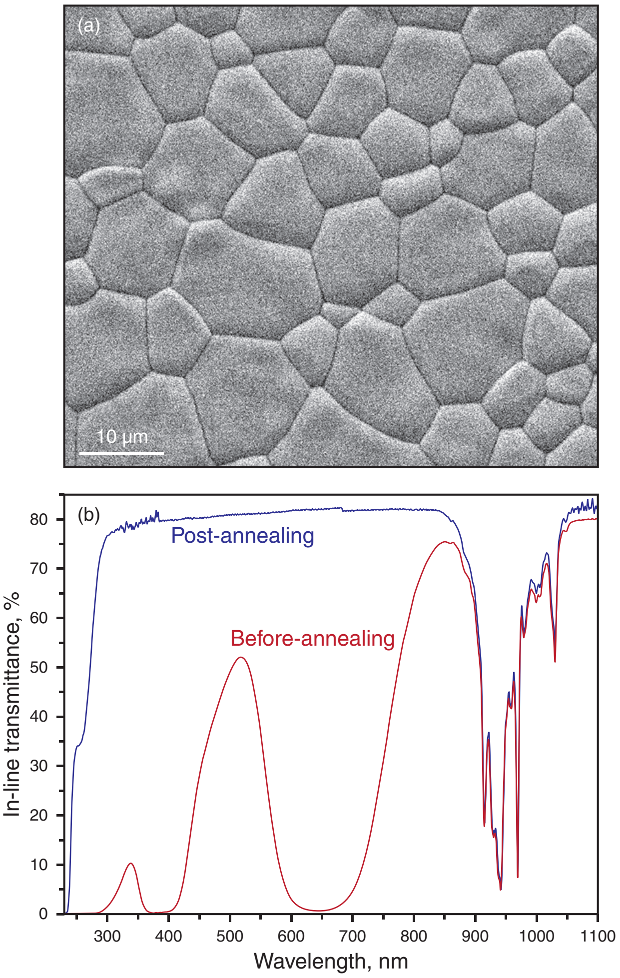

Figure 5 (online color at www.lasphys.com) (a) – SEM surface image and (b) – optical transmittance for the concentration gradient Yb:YAG composite ceramic

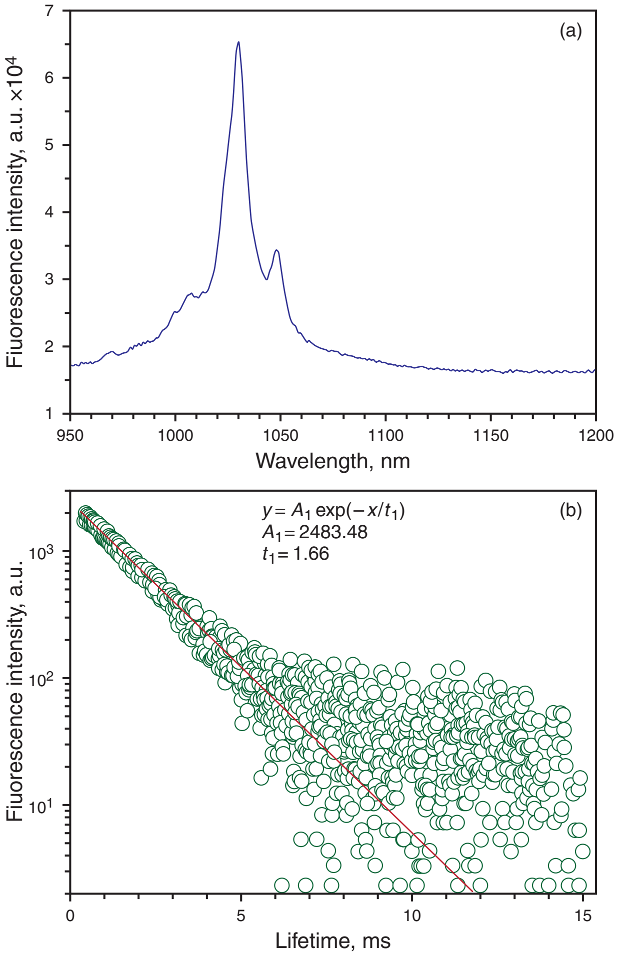

Figure 6 (online color at www.lasphys.com) (a) – fluorescence emission spectra and (b) – fitted fluorescence decay curve for the concentration gradient Yb:YAG composite ceramic

are colorless transparent. The color (green) fades gradually from the center to the edge, which is consistent with the variation of Yb concentration. The generation of green color can be attributed to the formation of F-color centers (e.g., Yb^{2+} ions and oxygen vacancy) during vacuum sintering [16] By annealing in oxygen atmosphere, the entire ceramic becomes colorless, as shown in Fig. 4b. The disappearance of green color indicates the elimination of F-color centers. Annealing treatment can not only eliminate the oxygen vacancy, but also promote the transformation of Yb^{2+} to Yb^{3+}, reducing Yb ions radium and allowing more Yb^{3+} ions to occupy Y^{3+} ions lattice sites. As a result, the lattice distortion would be relieved by annealing and thus crystal structure could be more perfect.

Fig. 5a shows scanning electron microscope (SEM) image of the annealed sample. The average grain size is about 10 μm, and no pores or second phase are observed. This full dense microstructure ensures high transmittance of the sample. As shown in Fig 5b, optical transmittance attains to 81% at the wavelength of 500 nm for the annealed specimen, and higher transmittance can be reached in infrared region. The strongest absorption peak is located at 940 nm, corresponding to the transition from $^2F_{7/2}$ to $^2F_{5/2}$ manifold of Yb^{3+} ions. For the unannealed sample, two additional large absorption peaks are also observed in visible region (located at 380 and 640 nm, respectively), which can be attributed to the formation of F-color centers, as discussed above. These two broadened adsorption peaks disappears after annealing treatment, which is in accordance with the color variation.

Fig 6a shows the fluorescence spectrum of the annealed ceramic. Two emission peaks, located at 1030 and 1049 nm respectively, are observed. Emission peak at 1030 nm is so strong that it permits population inversion more easily between laser energy levels. Fig. 6b shows the fitted fluorescence decay curve, and it is found that the

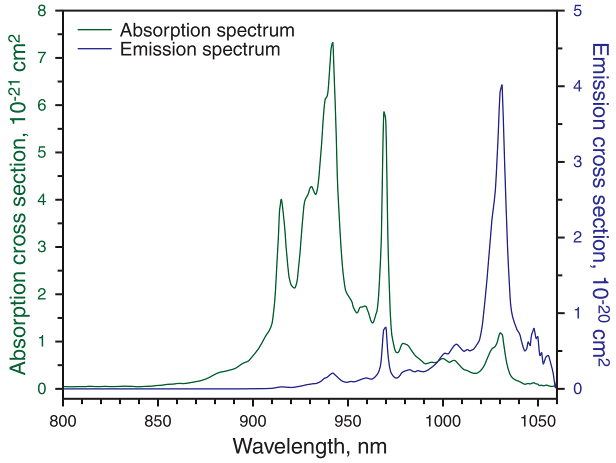

Figure 7 (online color at www.lasphys.com) Absorption and emission cross section for the concentration gradient Yb:YAG composite ceramic

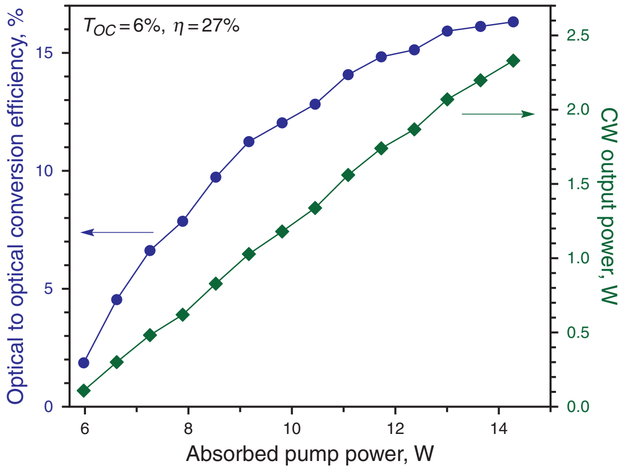

Figure 8 (online color at www.lasphys.com) CW laser output power (solid rhombus) and optical efficiency (solid circle) of the Yb:YAG gradient composite ceramic sample as a function of absorbed pump power

emission intensity at 1030 nm is decayed exponentially with time. The fluorescence lifetime is fitted to be 1.66 ms, which is comparable to that of our previous work [17]. This lifetime is longer than the theoretical value, which can be mainly attributed to the Yb^{3+} ions self-absorption effect around 1030 nm. Because of a large spectral overlap between the fluorescence and ground-state absorption exists (Fig. 7), photons that are spontaneously emitted from the metastable level are trapped by reabsorption by ions in the ground state. These nascent excited-state ions then relax by spontaneously emitting more photons, which are then reabsorbed, and the entire process is repeated. Consequently, the fluorescence lifetime is increased (compared with the lifetime of a single isolated ion) [18]. With increasing Yb^{3+} doping level, the ions slowly close to each other. Therefore, this effect is particularly serious at high Yb^{3+} doping concentration.

The absorption coefficient α is calculated according to the following equation: $\alpha = -\ln T\%/L$, where $T\%$ is the optical transmittance, and L is the ceramic thickness. Then, the absorption cross section σ_{abs} is determined using the equation: $\sigma_{abs} = \alpha/N$, where N is the mean concentration of Yb ions (cm^{-3}), and it is calculated to be 1.736×10^{21}cm^{-3} for this composite sample. The stimulated emission cross section σ_{em} of $^2F_{2/5}$ to $^2F_{7/2}$ is given by the reciprocity method: $\sigma_{em} = \sigma_{abs}\ Z_l/Z_u \exp[(E_{zl} - hc\lambda^{-1})/k_B T]$, where k_B is the Boltzmann constant, Z_l and Z_u represent the partition function of the ground and the excited multiplet, respectively. E_{zl} is the zero-line energy, which is defined as the energy separation between the lowest stark levels of the upper and lower multiplets. In the case of our composite sample, E_{zl} is 10327 cm^{-1}, and the ratio Z_l/Z_u is calculated to be 1.288. Fig. 7 shows the calculated σ_{abs} and σ_{em} spectra of $^2F_{5/2} \rightarrow {}^2F_{7/2}$ transition at room temperature. The maximum value of σ_{em} is 4.03×10^{-20} cm^2 at the wavelength of 1030 nm, which is comparable to the previous report [19].

Continuous wave (CW) laser performance at 1030 nm is demonstrated on the annealed sample by using 940 nm fiber-coupler diode laser as pumping source, and the obtained results are shown in Fig 8 When the transmission of output coupler (T_{oc}) is 6%, laser output power increases proportionally with increasing pump power. The threshold absorbed pump power is 5.9 W, and the slope efficiency reaches 27%. At the maximum absorbed pump power of 14.2 W, the output power attains to 2.33 W. It is also found that the optical efficiency increases with increasing pump power, and attains to the maximum value of 16.3% when the absorbed pump power is 14.2 W.

4. Conclusions

In conclusion, all-ceramic multilayer composite Yb:YAG laser materials have been successfully fabricated by the technique of both tape casting and simple vacuum sintering process The structure integrity of the sample was verified by EDAX and SEM studies. Full dense microstructure without pores or second phase was obtained, and the spectroscopic properties were also investigated CW laser performance was demonstrated on the composite sample by using 940 nm fiber-coupler diode laser. Slope efficiency of 27% for 6% T_{oc} and optical efficiency of 16.3% at the absorbed pump power of 14.2 W were achieved. The fine microstructure and laser output of such complex composite indicate that the technology of tape casting together with simple vacuum sintering could be a low-cost but efficient route for the fabrication of multilayer composite laser ceramic.

Acknowledgements This work was financially supported by the Key Program in Major Research Plan of National Natural Science Foundation of China (91022035), Hundred Talents Program of the Chinese Academy of Sciences, Main Direction Program of Knowledge Innovation of Chinese Academy of Sciences, and National High-tech R&D Program of China (863 Program).

References

[1] B.B. Zhou, Z.Y. Wei, Y.W. Zou, Y.D. Zhang, X. Zhong, G.L. Bourdet, and J.L. Wang, Opt. Lett. **35**, 288 (2010).
[2] J. Dong and K. Ueda, Laser Phys. Lett. **2**, 429 (2005).
[3] F. Tang, Y.G. Cao, W. Guo, Y.J. Chen, J.Q. Huang, Z.H. Deng, Z.G. Liu, and Z. Huang, Opt. Mater. **33**, 1278 (2011).
[4] Y.S. Wu, J. Li, Y.B. Pan, J.K. Guo, B.X. Jiang, Y. Xu, and J. Xu, J. Am. Ceram. Soc. **90**, 3334 (2007).
[5] L. Esposito, A. Piancastelli, J. Hostasa, T. Epicier, and G. Boulon, in: 7th Laser Ceramics Symposium: International Symposium on Transparent Ceramics for Photonic Applications, Singapore, November 14–17 2011 (7th LCS), p. 32.
[6] W. Strek, P. Gluchowski, L. Marciniak, and D. Hreniak, in: 7th Laser Ceramics Symposium: International Symposium on Transparent Ceramics for Photonic Applications, Singapore, November 14–17, 2011 (7th LCS), p. 80.
[7] F. Hanson, Appl. Phys. Lett. **66**, 3549 (1995).
[8] M. Tsunekane, N. Taguchi, and H. Inaba, Electron. Lett. **32**, 40 (1996).
[9] D. Kracht, R. Wilhelm, M. Frede, K. Dupré, and L. Ackermann, Opt. Express **13** 10140 (2005).
[10] K. Yoshida, A. Ikesue, and Y. Okamoto, in: Conference on Lasers and Electro Optics/International Quantum Electonics Conference, San Francisco, CA, USA, May 16–21, 2004 (CLEO/IQEC 2004), paper CTuT3
[11] Y. Sato, A. Ikesue, and T. Taira, IEEE J. Sel. Top. Quantum Electron. **13**, 838 (2007).
[12] T. Kamimura, T. Okamoto, Y.L. Aung, and A. Ikesue, in: Conference on Lasers and Electro Optics, Baltimore, MD, USA, May 6–11, 2007 (CLEO 2007), paper TThT6
[13] S.-H. Lee, E.R. Kupp, A.J. Stevenson, J.M. Anderson, G.L. Messing, X. Li, E.C. Dickey, J.Q. Dumm, V.K. Simonaitis-Castillo, and G.J. Quarles, J. Am. Ceram. Soc. **92**, 1456 (2009).
[14] N. Ter-Gabrielyan, L.D. Merkle, E.R. Kupp, G.L. Messing, and M. Dubinskii, Opt. Lett. **35** 922 (2010).
[15] F. Tang, Y.G. Cao, J.Q. Huang, H.G. Liu, W. Guo, and W.C. Wang, J. Am. Ceram. Soc. **95**, 56 (2011).
[16] X.D. Xu, Z.W. Zhao, P.X. Song, G.Q. Zhou, J. Xu, and P.Z. Deng, J. Opt. Soc. Am. B **21**, 543 (2004).
[17] F. Tang, J.Q. Huang, W. Guo, W.C. Wang, B.J. Fei, and Y.G. Cao, Opt. Mater. **34**, 757 (2011).
[18] D.S. Sumida and T.Y. Fan, Opt. Lett. **19**, 1343 (1994)
[19] J. Dong, A. Shirakawa, K. Ueda, H. Yagi, T. Yanagitani, and A.A. Kaminskii, Appl. Phys. Lett. **89**, 091114 (2006).